ELSEVIER

Journal of Crystal Growth 220 (2000) 316–325

JOURNAL OF CRYSTAL GROWTH

www.elsevier.nl/locate/jcrysgro

Axisymmetry breaking instabilities of natural convection in a vertical bridgman growth configuration

A.Yu. Gelfgat*, P.Z. Bar-Yoseph, A. Solan

Computational Mechanics Laboratory, Faculty of Mechanical Engineering, Technion Israel Institute of Technology, Haifa, 32000, Israel

Received 7 March 2000; accepted 15 August 2000
Communicated by J.J. Derby

Abstract

A study of the three-dimensional axisymmetry-breaking instability of an axisymmetric convective flow associated with crystal growth from bulk of melt is presented. Convection in a vertical cylinder with a parabolic temperature profile on the sidewall is considered as a representative model. The main objective is the calculation of critical parameters corresponding to a transition from the steady axisymmetric to the three-dimensional non-axisymmetric (steady or oscillatory) flow pattern. A parametric study of the dependence of the critical Grashof number Gr_{cr} on the Prandtl number $0 \leqslant Pr \leqslant 0.05$ (characteristic for semiconductor melts) and the aspect ratio of the cylinder $1 \leqslant A \leqslant 4$ (A = height/radius) is carried out. The stability diagram $Gr_{cr}(Pr, A)$ corresponding to the axisymmetric — three-dimensional transition is reported for the first time. The calculations are done using the spectral Galerkin method allowing an effective and accurate three-dimensional stability analysis. It is shown that the axisymmetric flow in relatively low cylinders tends to be oscillatory unstable, while in tall cylinders the instability sets in due to a steady bifurcation caused by the Rayleigh–Benard mechanism. The calculated neutral curves are non-monotonous and contain hysteresis loops. The strong dependence of the critical Grashof number and the azimuthal periodicity of the resulting three-dimensional flow indicate the importance of a comprehensive parametric stability analysis in different crystal growth configurations. In particular, it is shown that the first instability of the flow considered is always three-dimensional.

PACS: 81.10; 47.20

Keywords: Crystal growth; Hydrodynamic stability; Spectral methods

1. Introduction

Many bulk crystal growth processes are carried out in axisymmetric geometric configurations and under axisymmetric external conditions. However, the axisymmetric melt flows frequently become unstable and bifurcate to non-axisymmetric steady or oscillatory states. The instabilities of melt flow, lead to the appearance of temperature oscillations and asymmetric flow patterns which, in their turn, lead to inhomogeneities in the structure of the growing crystals (see Refs.[1–4] and references therein). Such axisymmetry-breaking instabilities of axisymmetric flows can be observed also in simple

* Corresponding author.
E-mail address: alexg@cmlp.technion.ac.il (A.Yu. Gelfgat).
http://tx.technion.ac.il/ ~ cml/cml/staff/alex.htm

0022-0248/00/$ - see front matter
PII: S0022-0248(00)00842-3

laboratory models (such as, e.g., convection in a cylinder heated from below) [5–11] that are usually considered in numerical studies [7,11–18]. The numerical simulation of such instabilities using various time-dependent three-dimensional solvers [15–22] is exceptionally CPU-time consuming. As a consequence of computer limitations, this is usually done on rather coarse grids. The alternative numerical approach, based on the linear stability analysis, allows one to avoid the straight-forward integration in time [11,14,18]. This approach considers all possible three-dimensional infinitesimal perturbations and usually provides better understanding of the instability phenomena as well as more precise critical values of the governing parameters. At the same time it requires the solution of a series of eigenproblems of very high order (the order is equal to the number of scalar unknowns of a numerical method). The difficulties and a possible numerical realization of such analysis are discussed in Ref. [23]. A comprehensive analysis of all possible instabilities yields a physical explanation of the experimentally observed phenomena of axisymmetry breaking (an example of that can be found in Ref. [11]). The detailed stability results obtained for hydrodynamic models of crystal growth devices will allow one to choose operating parameters that provide a stable melt flow pattern under the required technological conditions. Such an analysis remains a challenge. However, in our opinion, recent development of numerical methods and high-performance computing will make this possible in the near future. The present paper considers a simplified example to illustrate the type of results that can be expected in more complicated cases.

The numerical approach developed in Refs. [11,23] and devoted to the three-dimensional stability analysis of an arbitrary axisymmetric flow is used in the present study. This approach is still restricted to a simple cylindrical geometry but allows one to perform a detailed parametric investigation of stability taking into account *all* possible infinitesimally small perturbations. The present paper describes some preliminary results obtained for the stability of buoyant convection in a vertical cylinder with a *parabolic* temperature profile at the sidewall. We assume that the temperature of the top and bottom of the cylinder is at the melting point, while the most intensive heating takes place at the central part of the sidewall. Such heating is modeled by a parabolic temperature profile on the sidewall, which has a maximum at the midheight and vanishes to the melting point at the top and the bottom. This can be associated with a model of the vertical Bridgman [24–28] or liquid encapsulated melt zone [29] techniques. The stability diagrams showing the dependence of the critical Grashof number on the Prandtl number ($0 \leqslant \mathrm{Pr} \leqslant 0.05$) and the aspect ratio ($1 \leqslant H/R \leqslant 4$) of the cylinder are reported. The results obtained are in agreement with the previously published experimental and numerical data and show some qualitative tendencies of the axisymmetry–asymmetry transitions in low and tall cylinders having maximum of the temperature profile at the sidewall. Several characteristic patterns of the most dangerous perturbations are discussed. It is shown that the instability of the flow is three-dimensional for the whole range of governing parameters studied. Similar to our previous studies devoted to two-dimensional models [30,31], it is shown that the stability properties of a given flow cannot be completely understood without a detailed parametric study. In particular, it is not always possible to extrapolate a particular result to close but different values of the governing parameters. Such a strong dependence of the stability properties on the governing parameters indicates the necessity of a study of stability when a crystal growth device is being designed.

2. Formulation of the problem and numerical technique

We consider the convection of a Boussinesq fluid in a vertical cylindrical container of radius R and height H. The flow is described by the dimensionless three-dimensional Navier–Stokes, continuity and energy equations

$$\frac{\partial \boldsymbol{v}}{\partial t} + (\boldsymbol{v}\cdot\nabla)\boldsymbol{v} = -\nabla p + \Delta \boldsymbol{v} + \mathrm{Gr}T\boldsymbol{e}_z, \tag{1}$$

$$\nabla\cdot\boldsymbol{v} = 0, \tag{2}$$

$$\frac{\partial T}{\partial t} + (\boldsymbol{v}\cdot\nabla)T = \frac{1}{\mathrm{Pr}}\Delta T, \tag{3}$$

in the domain $0 \leqslant r \leqslant 1$, $0 \leqslant z \leqslant A$, $0 \leqslant \varphi \leqslant 2\pi$. Here $\boldsymbol{v} = \{v_r, v_\varphi, v_z\}$, T and p are non-dimensional velocity, temperature and pressure p, respectively. The dimensional scales of the time, the velocity and the pressure are R^2/ν, ν/R and $\rho(\nu/R)^2$, respectively. The temperature is non-dimensionalized as $T = (T^* - T_{\mathrm{melt}})/(T_{\max} - T_{\mathrm{melt}})$. Other parameters are: $\mathrm{Gr} = g\beta\Delta T H^3/\nu^2$, Grashof number, $\mathrm{Pr} = \nu/\chi$, Prandtl number, g acceleration due to gravity in the z-direction, β, thermal expansion coefficient, ν, viscosity, χ, heat diffusivity, and ρ, density. $T^*$is the dimensional temperature, $T_{\max}$ is the maximal temperature at the sidewall and T_{melt} is the melting temperature imposed at the top and the bottom.

It is assumed that the boundary conditions allow the existence of an axisymmetric steady solution of Eqs. (1)–(3). As an example we consider no-slip boundary conditions for velocity, a *parabolic* temperature profile at the sidewall of the cylinder and equal constant temperatures at the top and bottom. This reads

$$\text{At } z = 0 \text{ and } z = A: \quad T = 0, \qquad \boldsymbol{v} = \boldsymbol{0}, \tag{4}$$

$$\text{At } r = 1: \quad T = z(1 - z/A), \qquad \boldsymbol{v} = \boldsymbol{0}. \tag{5}$$

The boundary conditions at the axis should be added for the axisymmetric basic state flow

$$\text{At } r = 0: \quad \frac{\partial T}{\partial r} = 0, \quad v_r = 0, \quad v_\varphi = 0, \quad \frac{\partial v_z}{\partial r} = 0. \tag{6}$$

Note that the shape of the temperature profile at the sidewall is arbitrary and usually should be more complicated than a symmetric (with respect to the midheight) parabola defined in Eq. (5). The simplified temperature boundary conditions (5) is chosen here mainly for illustrative purposes.

To investigate the non-axisymmetric perturbations we use the 2π-periodicity of the solution of Eqs. (1)–(6) to represent it in the form

$$\{\boldsymbol{v}, p, T\} = \sum_{k=-\infty}^{k=\infty} \{\boldsymbol{v}_k, p_k, T_k\} \exp(\mathrm{i}k\varphi), \tag{7}$$

We are looking for values of the Grashof number for which the steady axisymmetric solution $\{\boldsymbol{v}_0(r,z), p_0(r,z), T_0(r,z)\}$ becomes unstable with respect to the axisymmetric ($k = 0$) or non-axisymmetric ($k \neq 0$) perturbations. The linear stability problem separates for each value of the azimuthal wavenumber k [11,23]. Therefore for each k one has to consider a quasi-axisymmetric problem which yields the critical Grashof number $\mathrm{Gr}_{\mathrm{cr}}(\mathrm{Pr}, A, k)$. Then the critical Grashof number is defined as $\mathrm{Gr}_{\mathrm{cr}}(\mathrm{Pr}, A) = \min_k \mathrm{Gr}_{\mathrm{cr}}(\mathrm{Pr}, A, k)$, and the value $k = k_{\mathrm{cr}}$ that corresponds to the minimum of $\mathrm{Gr}_{\mathrm{cr}}(\mathrm{Pr}, A, k)$ is the critical wavenumber. In the case of *oscillatory* instability the critical frequency of oscillations ω_{cr} (the oscillation frequency at $\mathrm{Gr} = \mathrm{Gr}_{\mathrm{cr}}$) should be added to the set of critical parameters. The dimensional scale for ω_{cr} is ν/R^2.

The calculations were carried out using the global Galerkin method described in Refs. [11,23]. Some details about the realization of the method for more complicated (but still axisymmetric) boundary conditions, including a finite heat conductivity of the sidewall, can be found in Ref. [11]. Test calculations for the classical Rayleigh–Benard problem in a finite vertical cylinder were performed in Ref. [13]. Additional tests for stability of the secondary axisymmetric flows in the Rayleigh–Benard configuration are described in Ref. [11]. To ensure the correctness of results a separate convergence study was performed for the boundary conditions (4)–(6). It showed that truncation of the Galerkin series to 30×30 basis functions in the r- and z-direction yields 3–4 correct digits in the critical Grashof number and the critical frequency.

3. Results

The patterns of the steady-state flows whose stability is studied are illustrated in Fig. 1. At all values of the aspect ratio considered the axisymmetric steady-state flow consists of a single toroidal convective roll. The fluid rises near the sidewall, where the temperature is maximal and descends along the axis. One can notice a significant change in the temperature distribution which happens with the increase of the aspect ratio. For the lowest aspect ratio considered ($A = 1$, Fig. 1a) strongly curved isotherms fill a large part of the flow region. At larger values of the aspect ratio (Figs. 1b and c) the curved isotherms, related to the temperature maximum at the sidewall, remain mostly in the central part of the cylinder. At the same time two

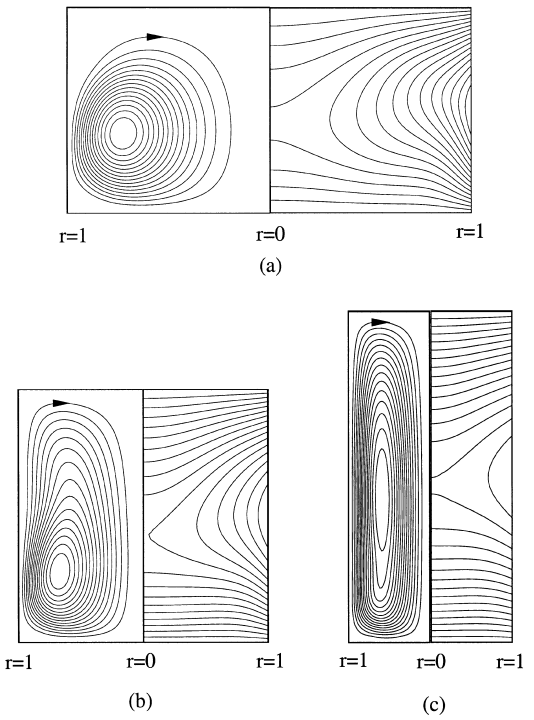

Fig. 1. Streamlines (left frame) and isotherms (right frame) of steady-state flows at the critical values of Grashof number. $\mathrm{Pr} = 0.015$. (a) $A = 1$, $\mathrm{Gr_{cr}} = 3.59 \times 10^5$, (b) $A = 2$, $\mathrm{Gr_{cr}} = 1.01 \times 10^5$, (c) $A = 4$, $\mathrm{Gr_{cr}} = 5.03 \times 10^4$.

stratified fluid layers develop near the top and the bottom. The stratification near the bottom (the cold fluid below the hot one) is stable, while stratification near the top (the cold fluid above the hot one) is unstable. The stability analysis (see below) shows, in particular, how the presence of stratified layers affects the stability properties of the flow.

First, we consider the dependence of the critical Grashof number on the Prandtl number for the fixed value of the aspect ratio $A = 1$. The stability diagram in Fig. 2a shows $\mathrm{Gr_{cr}}(\mathrm{Pr}, k)$ for $2 \leqslant k \leqslant 10$. The values of $\mathrm{Gr_{cr}}$ corresponding to $k = 0$ and 1 are larger than 10^6 and are not shown on the graph. At smaller values of the Prandtl number, for $0 \leqslant \mathrm{Pr} \leqslant 0.025$, the most dangerous mode corresponds to $k = 4$. At $\mathrm{Pr} \geqslant 0.025$ it is replaced by the $k = 3$ mode. The critical Grashof numbers, that correspond to the azimuthal modes with $k = 2$ and $k = 5$–10, are relatively close and grow rapidly with the increase of Pr. For low values of the Prandtl number ($\mathrm{Pr} < 0.02$) one can expect an interaction of several azimuthal modes at relatively large supercriticalities. For example, at $\mathrm{Pr} = 0.01$ the most dangerous mode with $k = 4$ is excited at $\mathrm{Gr_{cr}} \approx 3 \times 10^5$, then the $k = 2$ mode would be excited at $\mathrm{Gr} \approx 3.7 \times 10^5$ and at $\mathrm{Gr} \approx 4.5 \times 10^5$ many additional modes would be excited. This can lead to a quite complicated three-dimensional flow pattern. However, already for $\mathrm{Pr} \geqslant 0.025$ only modes with $k = 3$ and 4 can interact in the supercritical regime of a moderate supercriticality. A noticeable interaction of these modes can be expected for values of Pr close to 0.025, where both modes become unstable simultaneously. Both bifurcations corresponding to $k = 3$ and 4 at $A = 1$ are transitions from a steady axisymmetric to an oscillatory three-dimensional flow via the Hopf bifurcation. The critical circular frequencies (i.e., frequencies of oscillations at the critical value of Gr) corresponding to these two modes are shown in Fig. 2b.

Calculations for fixed values of the Prandtl number and varying aspect ratio were carried out for $\mathrm{Pr} = 0$, 0.015, 0.03 and 0.05 and $1 \leqslant A \leqslant 4$. An example of the stability diagram for $\mathrm{Pr} = 0.015$ and $0 \leqslant k \leqslant 6$ is shown in Fig. 3. It is seen that behavior of the curves $\mathrm{Gr_{cr}}(A, k)$ is rather complicated and detailed parametric calculations are required to complete the study. Thus, the stability diagram shown in Fig. 3 contains more than 600 calculated bifurcation points. Obviously, only the lower envelope of the curves $\mathrm{Gr_{cr}}(A, k)$ is of practical interest. However, all the curves have to be calculated to reach the final result.

The results containing only *the lower envelopes of the curves* $\mathrm{Gr_{cr}}(A, k)$ for different Prandtl numbers are collected in Fig. 4. The critical azimuthal wavenumbers are shown for each particular branch of the neutral curves. All curves, except the one corresponding to $\mathrm{Pr} = 0$ (i.e., neglected convection of heat) behave similarly. This indicates the importance of the convective heat transfer for the onset of the instability even for Prandtl numbers of order 10^{-2}. The critical Grashof numbers, corresponding to $\mathrm{Pr} \neq 0$, decrease with the increase of the aspect ratio and have rather close values in the interval $1.3 \leqslant A \leqslant 2.5$. At larger values of A the critical curves start to diverge showing hysteretic behavior.

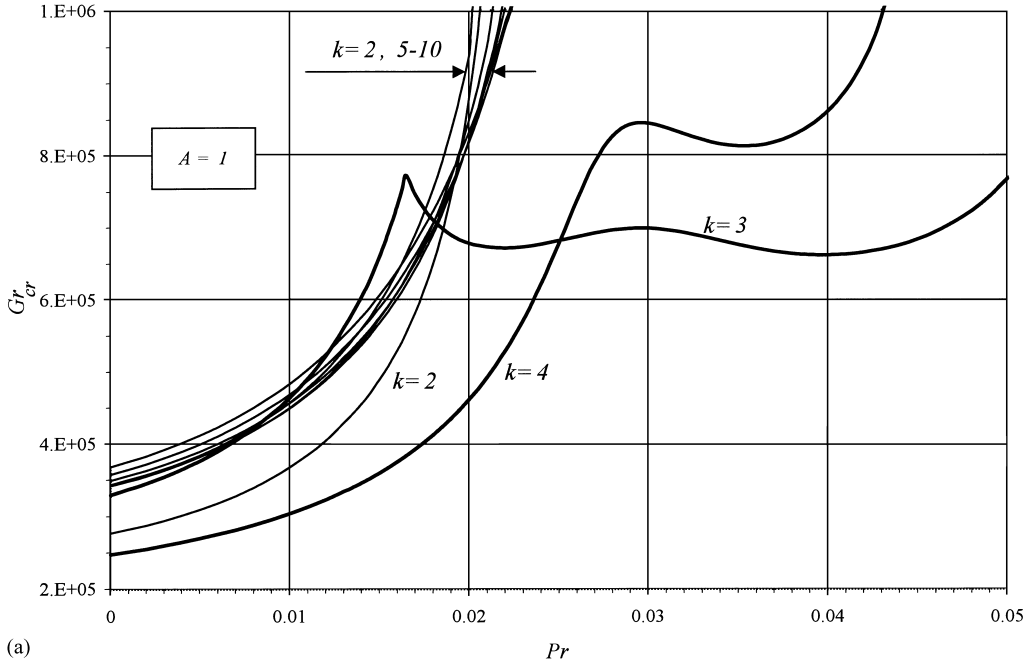

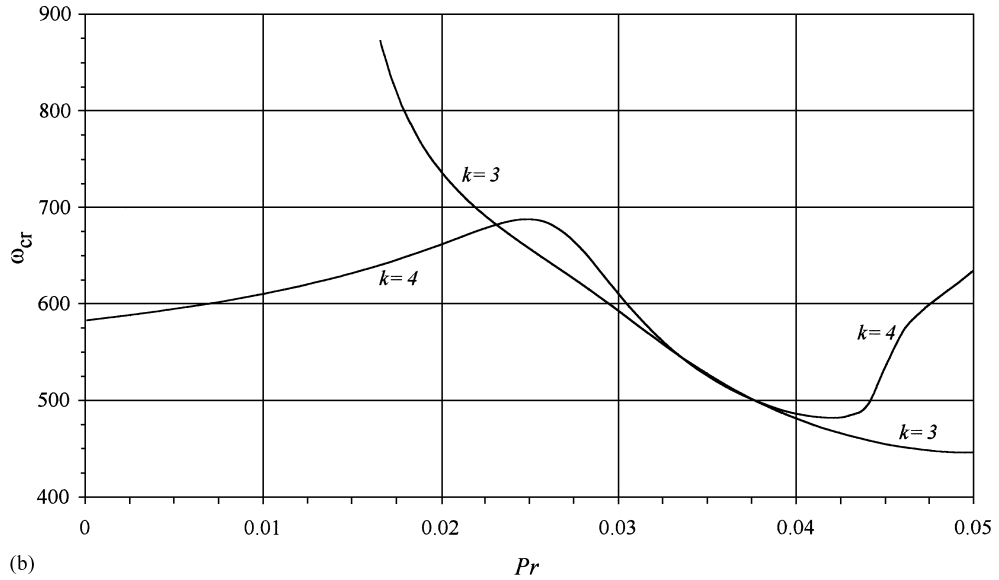

Fig. 2. (a) Dependence of the critical Grashof number on the Prandtl number for the fixed aspect ratio $A = 1$ and different azimuthal wavenumbers k. (b) Dependence of the critical circular frequency on the Prandtl number for the two most dangerous azimuthal modes $k = 3$ and 4.

With the increase of the Prandtl number the location of the hysteresis loop moves towards smaller values of the aspect ratio. Knowledge about the exact location of the hysteresis loops can be important from a practical viewpoint. Thus, at $\mathrm{Pr} = 0.015$ and $A = 4$ (Fig. 4) the first instability

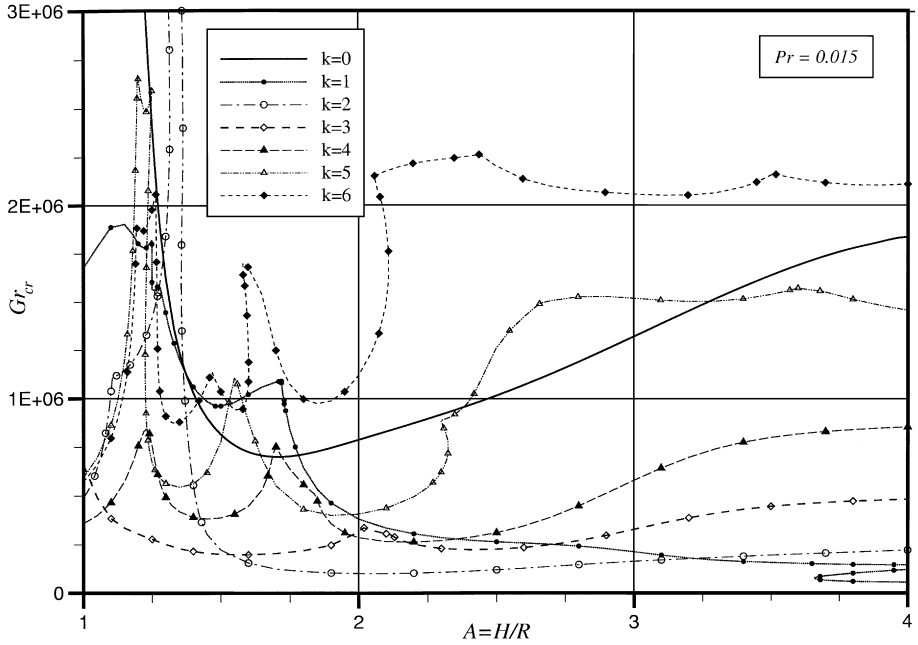

Fig. 3. Critical Grashof numbers $\mathrm{Gr}_{cr}(A,k)$ for $1 \leqslant A \leqslant 4$, $0 \leqslant k \leqslant 6$ and $\mathrm{Pr} = 0.015$.

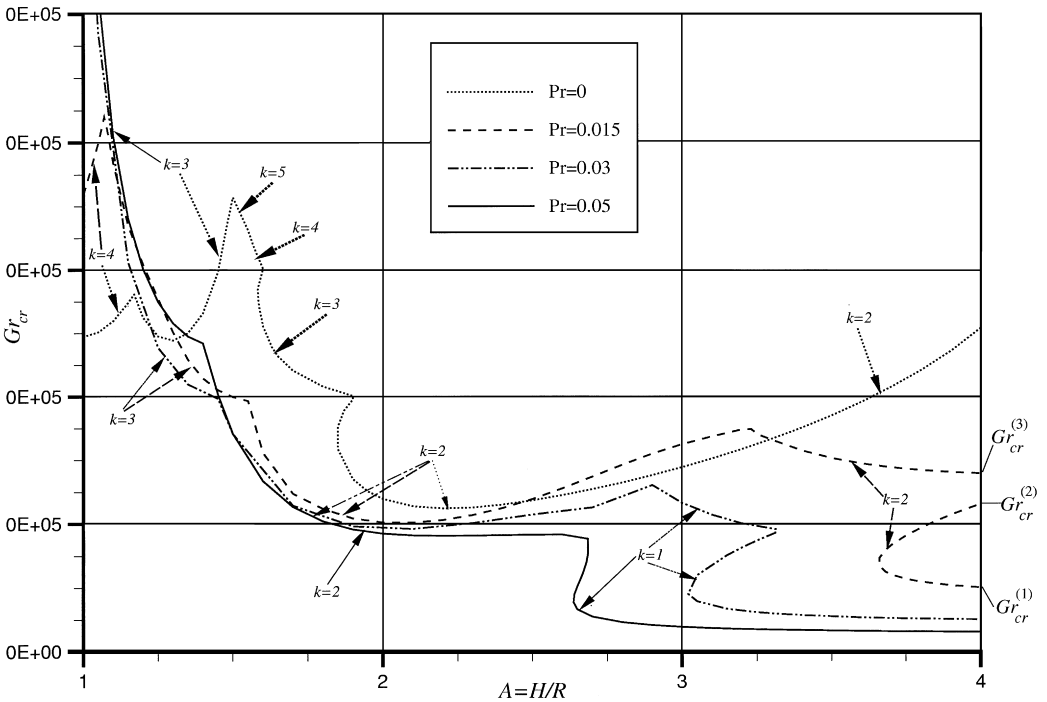

Fig. 4. The lower envelopes of the curves $\mathrm{Gr}_{cr}(A,k)$ for $1 \leqslant A \leqslant 4$ and different Prandtl numbers.

sets in at $Gr_{cr}^{(1)} \approx 5.03 \times 10^4$. The axisymmetric steady flow remains unstable until the Grashof number exceeds the next critical value $Gr_{cr}^{(2)} \approx 1.15 \times 10^5$. Then the axisymmetric steady flow becomes stable until the next critical number $Gr_{cr}^{(3)} \approx 1.39 \times 10^5$ will be exceeded. Therefore, the flow can be kept stable in the interval $Gr_{cr}^{(2)} \leqslant Gr \leqslant Gr_{cr}^{(3)}$ at more than twice larger Grashof number (temperature difference) than $Gr_{cr}^{(1)}$. Note that in the considered model the axisymmetric mode $k = 0$ never becomes critical. This shows the necessity to use three-dimensional models for calculations in the supercritical regimes.

The case $Pr = 0.02$ and $A = 2$ was studied numerically in Ref. [19] by a straightforward integration in time. The critical Grashof number was estimated in these calculations as $Gr_{cr} \approx 1.25 \times 10^5$ (the Rayleigh number Ra_w defined in Ref. [19] should be rescaled as $Gr = Ra_w/2A^4$). The corresponding critical Grashof number calculated in the present study is slightly below 10^5 (see Fig. 4). This is a rather good comparison, since the straightforward calculation of Ref. [19] can indicate only instability with a finite amplitude, while the present linear stability analysis provides critical numbers corresponding to the infinitesimally small amplitude perturbations. Therefore, the present result should, indeed, be slightly smaller than the corresponding result of Ref. [19].

Some additional understanding on how the instability sets in can be drawn from the patterns of the most dangerous perturbation. Generally, each continuous branch of each neutral curve shown in Fig. 4 should be characterized by its own perturbation pattern, which is defined by the eigenvector of the linearized stability problem [23]. Some of the patterns, corresponding to different Pr and equal k_{cr} are similar (e.g., for $A = 2$, $k_{cr} = 2$ the perturbation patterns are similar for all values of the Prandtl number considered), but most of them are not. Generally, the eigenvector is a complex function. However, the problem considered is symmetric with respect to the change of the sign of φ. Therefore, the sign of k_{cr} is arbitrary and the most general expression for the perturbation is

$$\varepsilon\{E(r,z)\exp[\mathrm{i}(\omega_{cr}t + k_{cr}\varphi)] + \bar{E}(r,z)\exp[-\mathrm{i}(\omega_{cr}t + k_{cr}\varphi)]\}, \tag{8}$$

where ε is an unknown small amplitude, $E(r,z)$ is the eigenvector and the overbar denotes the complex conjugate. The real function defined by Eq. (8) is used here to plot the pattern of the temperature perturbation (see Refs. [11,23] for details).

Fig. 5 illustrates the three most characteristic patterns of the temperature perturbation found in the present study. The two perturbation patterns shown in Figs. 5a and b correspond to the

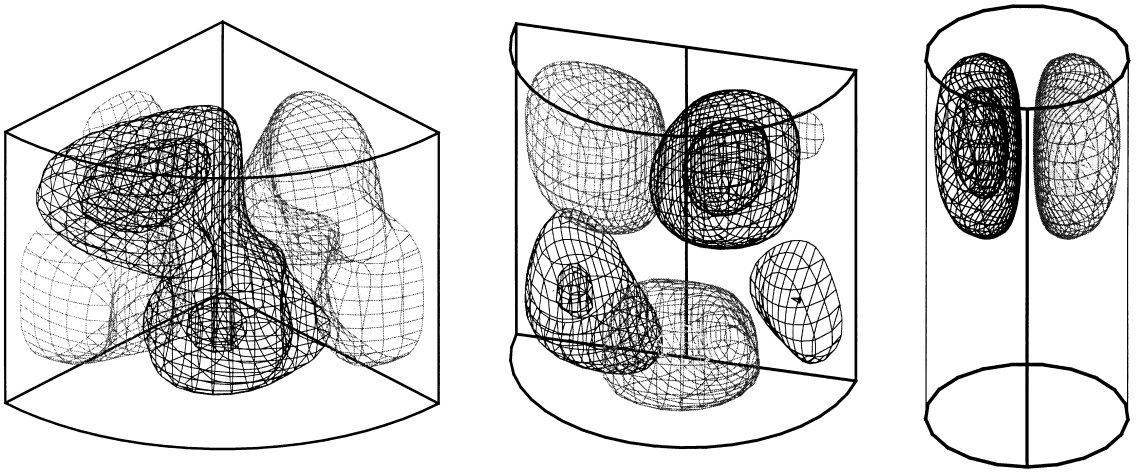

Fig. 5. Isosurfaces of the perturbation of the temperature. (a) $A = 1$, $Pr = 0.015$, $Gr_{cr} = 3.59 \times 10^5$, $k_{cr} = 4$, $\omega_{cr} = 632.2$; (b) $A = 2$, $Pr = 0.03$, $Gr_{cr} = 9.6 \times 10^4$, $k_{cr} = 2$, $\omega_{cr} = 157.3$; (c) $A = 4$, $Pr = 0.03$, $Gr_{cr} = 2.55 \times 10^4$, $k_{cr} = 1$, $\omega_{cr} = 0$.

transition from the steady axisymmetric to the oscillatory non-axisymmetric flow due to the Hopf bifurcation. The critical circular frequencies are 632.2 and 157.3, respectively. The physical meaning of the bifurcation patterns can be understood if we represent the supercritical oscillatory flow as a sum of the constant averaged and the oscillatory components. At low supercriticalities the averaged component is axisymmetric, while the oscillatory component coincides with Eq. (8) to within multiplication by a complex constant. The patterns of perturbations (Figs. 5a and b) correspond to Eq. (8) at $t = 0$ and provide an illustration of the oscillatory component of the slightly supercritical oscillatory three-dimensional flow ($t \neq 0$ leads only to a shift of the pattern in the azimuthal direction). The levels of the isosurfaces are equally distributed from the minimal to maximal values. The darker color corresponds to larger values. It should be noted that in the case of Hopf bifurcation, i.e. $\omega_{cr} \neq 0$, the three-dimensional perturbation (8) has the form of a traveling wave. Therefore the oscillatory perturbation patterns (as well as the oscillatory component of the flow) rotate around the axis with the angular velocity ω_{cr}/k_{cr} .

Comparing Figs. 5a and b one can see a clear difference in the distribution of the amplitude of three-dimensional oscillations in shorter (Fig. 5a, $A = 1$) and taller (Fig. 5b, $A = 2$) cylinders. In the case $A = 1$ (Fig. 5a) the large-amplitude oscillations are distributed over the almost whole meridional plane. A similar perturbation pattern is characteristic for the case $\mathrm{Pr} = 0$. Therefore, the instability has a pure hydrodynamic origin and can be related to the instability of the circulating flow. In the case $A = 2$ the strongest oscillations are located in the higher part of the cylinder and can be associated with the developing of the unstably stratified fluid layer (Fig. 1b). Possibly, the oscillatory axisymmetry-breaking instability in this case is affected by the Rayleigh–Benard mechanism.

At larger values of the aspect ratio the oscillatory instability is replaced by a steady bifurcation with $k_{cr} = 1$. The characteristic pattern of the temperature perturbation is shown in Fig. 5c. In the case of a steady axisymmetry-breaking bifurcation the physical meaning of the perturbation pattern cannot be associated with the oscillatory part of the flow. Here the perturbation shows only the exponentially growing function whose pattern has the same azimuthal symmetry as the resulting three-dimensional flow. As illustrated in Fig. 5c the temperature perturbation has two extrema located inside the unstably stratified fluid layer (see Fig. 1c). The pattern of the velocity perturbation (not shown here) indicates the development of two antisymmetric rolls inside the layer. Obviously, this should be associated with the Rayleigh–Benard instability of the unstably stratified layer. Note that the transition due to the Rayleigh–Benard instability is always a steady pitchfork bifurcation, as is the case here. The pitchfork is defined by the arbitrary sign of $\pm k_{cr}$, such that the direction of fluid motion in each of the Rayleigh–Benard rolls is defined with the probability of $\frac{1}{2}$. Moreover, in the cylinders heated from below the Rayleigh–Benard instability sets in as an axisymmetry-breaking steady bifurcation with $k_{cr} = 1$ [12,14], exactly as it is observed here. However, the appearance of the hysteresis loops on the neutral curves is not usual for the Rayleigh–Benard instability. Possibly, the hysteretic behavior is caused by the interaction of the secondary Rayleigh–Benard rolls with the main convective roll or with the lower stably stratified layer. The latter should cause a stabilizing effect.

4. Concluding remarks

The simplified model presented here was used as an illustration of results that a comprehensive stability study can yield for practical purposes. As was already mentioned the numerical technique used is not restricted to a specific set of boundary conditions and can be applied for three-dimensional stability analysis of *any* axisymmetric flow in a cylindrical vessel. However, some general qualitative conclusions can be drawn from the results presented. First, the critical Grashof number, as well as the critical frequency of oscillations and the critical azimuthal wavenumber, strongly depend on the governing parameters of the problem. This repeats the conclusions made in our previous two-dimensional stability studies [30,31]. Generally, for a certain convective flow no estimations of the critical numbers or azimuthal periodicity can be

extrapolated from consideration of a similar model or close values of the Prandtl number and aspect ratio. A similar strong dependence on the boundary conditions also can be found [20]. Therefore, the critical values should be calculated for each particular case using as precise as possible, boundary conditions and values of governing parameters. Since the mathematical models used to describe the crystal growth processes usually are not very precise, the calculation of a comprehensive stability diagram, which shows parametric dependencies, can be very important and cannot be replaced by several unconnected critical points. It is also noticeable that the axisymmetric instability mode was not found to be critical in the whole range of parameters considered. Therefore, the numerical modeling of supercritical flow regimes should be always done in the three-dimensional formulation.

Comparison of the present result with the experimental results of Ref. [9] allows us to note a certain qualitative tendency for cases when the temperature profile on the sidewall has a single maximum. The temperature boundary conditions on the sidewall in Ref. [9] differed from Eq. (5), but the sidewall temperature profile also had a maximum in the middle of the wall and decreased to a minimum towards the top and the bottom. In Ref. [9] the temperature was uniform (hot) over a region near midheight of the sidewall, whose upper and lower parts were thermally insulated. The experimental results of Ref. [9] showed that the axisymmetry-breaking transition happens as a steady bifurcation with $k_{cr} = 1$ in the cylinders with $A > 3$ and as an oscillatory instability in cylinders with $A < 3$. This qualitatively agrees with the present results. Moreover, larger azimuthal asymmetry of the temperature profile was observed in the upper part of the cylinder, which also indicates the Rayleigh–Benard instability in the upper unstably stratified fluid layer. Therefore, we assume that in the relatively short cylinders the axisymmetry-breaking instability tends to be oscillatory, while in tall cylinders one should expect a steady bifurcation caused by the Rayleigh–Benard instability of the unstably stratified fluid layer. As was mentioned, the exact values of critical Grashof numbers strongly depend on the governing parameters and on boundary conditions and therefore should be calculated for each case separately. Note also that in the vertical Bridgman growth devices the Grashof number usually is of order 10^5–10^6 [24–28], which corresponds to the range of critical Grashof numbers obtained here.

Acknowledgements

This work was supported by the Israel Ministry of Science (Grant 8575-1-98), the Israel Ministry of Immigrant Absorption (to A.Gelfgat), the Israel High Performance Computer Unit, the Fund for Promotion of Research and the Y.Winograd Chair of Fluid Dynamics and Heat Transfer at Technion.

References

[1] G. Müller, Convective instabilties in melt growth configurations, J. Crystal Growth 128 (1993) 26.
[2] K. Kakimoto, Flow instability during crystal growth from the melt, Prog. Crystal Growth Charact. 30 (1995) 191.
[3] K. Kakimoto, Heat and mass transfer in semiconductor melts during single-crystal growth processes, Appl. Phys. Rev. 77 (1995) 1827.
[4] S. Nakamura, M. Eguchi, T. Azami, T. Hibiya, Thermal waves of a non-axisymmetric flow in a Czochralski-type silicon melt, J. Crystal Growth 207 (1999) 55.
[5] J.M. Olson, F. Rosenberger, Convective instabilities in a closed vertical cylinder heated from below. I. Monocomponent gases, J. Fluid Mech. 92 (1979) 609.
[6] K.R. Kirchartz, U. Müller, H. Oertel, J. Zierep, Axisymmetric and non-axisymmetric convection in a cylindrical container, Acta Mech. 40 (1981) 182.
[7] G. Müller, G. Neumann, W. Weber, Natural convection in vertical Bridgman configuration, J. Crystal Growth 70 (1984) 78.
[8] Y. Kamotani, F.-B. Weng, S. Ostrach, J. Platt, Oscillatory natural convection of a liquid metal in circular cylinders, J. Heat Transfer 116 (1994) 627.
[9] R. Selver, Y. Kamotani, S. Ostrach, Natural convection of a liquid metal in vertical cylinders heated locally from the side, J. Heat Transfer 120 (1998) 108.
[10] B. Hof, P.G.J. Lucas, T. Mullin, Flow state multiplicity in convection, Phys. Fluids 11 (1999) 2815.
[11] A.Yu. Gelfgat, P.Z. Bar-Yoseph, A. Solan, T. Kowalewski, Axisymmetry-breaking bifurcations in axially symmetric natural convection, Int. J. Transport Phenomena 1 (1999) 173.
[12] G. Neumann, Three-dimensional numerical simulation of buoyancy-driven convection in vertical cylinders heated from below, J. Fluid Mech. 214 (1990) 559.
[13] A. Yu. Gelfgat, I. Tanasawa, Systems of basis functions for calculation of three-dimensional fluid flows in cylindrical containers with the Galerkin spectral method, Proceedings

of Institute of Industrial Science, The University of Tokyo, Vol. 45, 1993, p. 60.
[14] M. Wanschura, H.C. Kuhlmann, H.J. Rath, Three-dimensional instability of axisymmetric buoyant convection in cylinders heated from below, J. Fluid Mech. 326 (1996) 399.
[15] Y.H. Li, K.C. Lin, T.F. Lin, Computation of unstable liquid metal convection in a vertical closed cylinder heated from the side and cooled from above, Numer. Heat Transfer. Part A. 32 (1997) 289.
[16] R. Verzicco, R. Camussi, Transitional regimes of low-Prandtl thermal convection in a cylindrical shell, Phys. Fluids 9 (1997) 1287.
[17] H. Ben Hadid, D. Henry, R. Touihri, Unsteady three-dimensional buoyancy-driven convection in a circular cylindrical cavity and its damping by magnetic field, J. Crystal Growth 180 (1997) 433.
[18] R. Touihri, H. Ben Hadid, D. Henry, On the onset of convective instabilities in cylinrical cavities heated from below, I. Pure thermal case, Phys. Fluids 11 (1999) 2078.
[19] J. Baumgartl, W. Budweiser, G. Müller, G. Neumann, Studies of buoyancy driven convection in a vertical cylinder with parabolic temperature profile, J. Crystal Growth 97 (1989) 9.
[20] G. Barwölff, F. König, G. Seifert, Thermal buoyancy convection in vertical zone melting configurations, Zeitschrift für Mathematik und Mechanik 10 (1997) 757.
[21] T. Kaiser, K.W. Benz, Floating-zone growth of silicon in magnetic fields. III. Numerical simulation, J. Crystal Growth 183 (1998) 564.
[22] G. Kasperski, A. Batoul, G. Labrosse, Up to the unsteadiness of axisymmetric thermocapillary flows in a laterally heated liquid bridge, Phys. Fluids 12 (2000) 103.
[23] A. Yu. Gelfgat, Two- and three-dimensional instabilities of confined flows: numerical study by a global Galerkin method. Proceedings of the 8th International Symposium on Computational Fluid Dynamics, Bremen, Germany, 5–10 September 1999, pp. 122–150 (to appear in Comput. Fluid Dyn. Journal).
[24] M.J. Crochet, F. Dupret, Y. Ryckmans, F.T. Geyling, E.M. Monberg, Numerical simulation of crystal growth in a vertical Bridgman furnace, J. Crystal Growth 97 (1989) 173.
[25] J.J. Favier, Recent advances in Bridgman growth modelling and fluid flow, J. Crystal Growth 99 (1990) 18.
[26] G. Müller, A. Ostrogorsky, Convection in melt growth, in: Handbook of Crystal Growth, Vol. 2b, Elsevier, Amsterdam, 1994, p. 709.
[27] J.P. Garandet, T. Albousiérre, Bridgman growth: modelling and experiments, Prog. Crystal Growth Charact. Mater. 38 (1999) 73.
[28] V.M. Lakeenkov, V.B. Ufimtsev, N.I. Shmatov, Yu.F. Schelkin, Numeric simulation of vertical Bridgman growth of $Cd_{1-x}Zn_xTe$ melts, J. Crystal Growth 197 (1999) 443.
[29] C.R. Lopez, J.R. Mileham, R. Abbaschian, Microgravity growth of GaSb single crystals by the liquid encapsulated melt zone (LEMZ) technique, J. Crystal Growth 200 (1999) 1.
[30] A.Yu. Gelfgat, P.Z. Bar-Yoseph, A. Solan, Vortex breakdown and instability of swirling flow in a cylinder with rotating top and bottom, Phys. Fluids 8 (1996) 2614.
[31] A.Yu. Gelfgat, P.Z. Bar-Yoseph, A.L. Yarin, Stability of multiple steady states of convection in laterally heated cavities, J. Fluid Mech. 388 (1999) 315.